Coxiella burnetii actively blocks IL-17-induced oxidative stress in macrophages

Tatiana M. Clemente, Leonardo Augusto, Rajendra K. Angara, and Stacey D. Gilk

Department of Pathology and Microbiology, University of Nebraska Medical Center, Omaha, NE, US

*Corresponding author
Stacey D. Gilk
University of Nebraska Medical Center
985900 Nebraska Medical Center
DRCII 5031
Omaha, NE 68198-5900
E-mail: sgilk@unmc.edu

Keywords: *Coxiella,* intracellular pathogen, IL-17 signaling, immune response.

Abstract

Coxiella burnetii is a highly infectious pathogen that causes Q fever, a leading cause of culture-negative endocarditis. *Coxiella* first targets alveolar macrophages and forms a phagolysosome-like compartment called the *Coxiella*-Containing Vacuole (CCV). Successful host cell infection requires the Type 4B Secretion System (T4BSS), which translocates bacterial effector proteins across the CCV membrane into the host cytoplasm, where they manipulate numerous cell processes. Our prior transcriptional studies revealed that *Coxiella* T4BSS blocks IL-17 signaling in macrophages. Given that IL-17 is known to protect against pulmonary pathogens, we hypothesize that *C. burnetii* T4BSS downregulates intracellular IL-17 signaling to evade the host immune response and promote bacterial pathogenesis. Using a stable IL-17 promoter reporter cell line, we confirmed that *Coxiella* T4BSS blocks IL-17 transcription activation. Assessment of the phosphorylation state of NF-κB, MAPK, and JNK revealed that *Coxiella* downregulates IL-17 activation of these proteins. Using ACT1 knockdown and IL-17RA or TRAF6 knockout cells, we next determined that IL17RA-ACT1-TRAF6 pathway is essential for the IL-17 bactericidal effect in macrophages. In addition, macrophages stimulated with IL-17 generate higher levels of reactive oxygen species, which is likely connected to the bactericidal effect of IL-17. However, *C. burnetii* T4SS effector proteins block the IL-17-mediated oxidative stress, suggesting that *Coxiella* blocks IL-17 signaling to avoid direct killing by the macrophages.

Importance

Bacterial pathogens are constantly evolving mechanisms to modulate the hostile host environment encountered during infection. *Coxiella burnetii,* the causative agent of Q fever, is a fascinating example of intracellular parasitism. *Coxiella* survives in a phagolysosome-like vacuole and uses the Dot/Icm type IVB secretion system (T4BSS) to deliver bacterial effector proteins into the host cell cytoplasm to manipulate several host cell functions. We recently demonstrated that *Coxiella* T4BSS blocks the IL-17 signaling in macrophages. Here, we found that *Coxiella* T4BSS inhibits IL-17 activation of the NF-κB and MAPK pathways and blocks IL-17-mediated oxidative stress. These findings reveal a novel strategy employed by intracellular bacteria to escape the immune response

during initial stages of infection. Further identification of virulence factors involved in this mechanism will bring to light new therapeutic targets to prevent Q fever development into a chronic life-threatening endocarditis.

Introduction

Q fever, caused by the highly infectious bacterium *Coxiella burnetii,* is a debilitating and potentially fatal disease considered a major public health problem worldwide [1, 2]. Acute Q fever most commonly manifests as a debilitating flu-like illness, but the infection can develop into a life-threatening endocarditis in chronic cases [3]. Q fever endocarditis requires up to 24 months of antibiotics combination therapy, surgical valve replacement can be needed, and lack of treatment has a high mortality rate [4-9]. Further, the only vaccine available for humans is licensed exclusively in Australia due to reactivity issues [10]. Between 2007 and 2010, the Netherlands experienced a large Q fever outbreak with more than 40,000 individuals infected [11], with smaller outbreaks occurring in the US [12-14], Spain [15], Australia [15], Japan [16] and Israel [17]. These outbreaks exemplify how expansive *C. burnetii* is globally, but the scarcity of prevention and treatment options is due to our lack of understanding of *C. burnetii* pathogenesis.

C. burnetii is an obligate intracellular pathogen that primarily targets alveolar macrophages during natural infection. Intracellularly, *C. burnetii* promotes formation of a phagolysosome-like *C. burnetii*-Containing Vacuole (CCV) which supports bacterial replication. Within the CCV, *C. burnetii* uses the specialized Dot/Icm type IVB secretion system (T4BSS) to deliver bacterial proteins into the host cell cytoplasm to manipulate host signaling pathways. Besides maintaining CCV fusogenicity with the endocytic pathway, T4BSS effectors block apoptosis and prevent pyroptosis by inhibiting inflammasome activation [18, 19]. However, how *C. burnetii* evades the host innate immune response and establishes chronic infection is still unclear. Our previous transcriptome analysis of infected alveolar macrophages identified IL-17 signaling as one of the top pathways manipulated by *C. burnetii* T4BSS effector proteins at early stages of infection [20]. IL-17 is a proinflammatory cytokine that plays a key role in protecting the host from infection by both extracellular and intracellular pulmonary pathogens [21-25]. In the lung, IL-17 is secreted by Th17 cells, γδ T cells and NK T cells, and acts on a

variety of cells due to its ubiquitous receptor [26-28]. In macrophages, IL-17 upregulates antimicrobial peptides, chemokine secretion, neutrophil recruitment, and activation of Th1 response, thus leading to pathogen killing [29-32]. However, we found that *C. burnetii* T4BSS downregulates expression of IL-17 host target genes, blocks IL-17-stimulated chemokine secretion, and confers protection from the IL-17 bactericidal effect [20]. These surprising findings suggest that *C. burnetii* downregulates IL-17 signaling through T4BSS effector proteins to subvert the immune response and promote bacterial survival.

IL-17 signals through a dimeric IL-17RA and IL-17RC receptor complex, which triggers multiple intracellular signaling pathways, with the signaling adaptor Act1 (also known as CIKS - Connection to IKK and SAPK/JNK), required for all known IL-17-dependent signaling pathways [24, 33, 34]. Of note, the physical association between two IL-17R subunits is absolutely required for IL-17 signaling, given that a lack of either IL-17RA or IL-17RC completely abolishes the receptor function [35, 36]. Upon ligand binding, Act1 interacts with IL-17 receptor through the conserved SEFIR (Similar Expression of Fibroblast growth factor and IL-17R) domain and activates several independent signaling pathways mediated through different TRAF proteins [37, 38]. Unphosphorylated ACT1 ubiquitinates TRAF6, which activates the NF-κB and MAPK pathways and transcription of inflammatory genes, including *il6, tnfa, cxcl2, cxcl5 and ccl2* [24]. In contrast, phosphorylated ACT1 associates with TRAF2/5, and the complex ACT1/TRAF2/5 binds to the 3' mRNA of IL-17-target genes and stabilizes the mRNA for translation [24]. While there is evidence that the *C. burnetii* T4BSS manipulates NF-κB and MAPK signaling pathways [39-41], upstream pathways such as IL-17 have not been explored. Of note, increased IL-17 levels were detected following *C. burnetii* stimulation of peripheral blood mononuclear cells (PBMCs) from both healthy and chronic Q fever patients [42, 43]. *In vitro* data demonstrating that *C. burnetii* inhibits intracellular IL-17 signaling [20] supports an *in vivo* finding that *C. burnetii*-infected IL-17 receptor knockout mice had a similar bacterial burden in the spleen and lung as infected wildtype mice [44].

In the current study, we demonstrate that *C. burnetii* T4BSS blocks the transcription pathway activated by IL-17, and disruption of the IL17R-ACT1-TRAF6 pathway neutralizes the IL-17 bactericidal effect. Furthermore, alveolar macrophages produce higher levels of reactive oxygen species (ROS) in response to IL-17, but *C. burnetii*

T4BSS effector proteins completely inhibit the IL-17-mediated oxidative stress. Together, our data suggests that *C. burnetii* T4BSS downregulates IL-17 signaling in macrophages to avoid being directly killed by oxidative stress.

Results

C. burnetii T4BSS blocks activation of IL-17 signaling in alveolar macrophages.

Our previous transcriptome analysis revealed IL-17 signaling as a primary target of *C. burnetii* during the early stages of macrophage infection, with the *C. burnetii* T4BSS downregulating expression of IL-17 host target genes [20]. Therefore, we hypothesized that *C. burnetii* T4BSS effector proteins block the ACT1/TRAF6 pathway downstream of the IL-17 receptor. To measure activation of the IL-17 transcription pathway during *C. burnetii* infection, we used a stable IL-17 promoter reporter cell line (HEK-Blue™ IL-17 cells; InvivoGen). HEK-Blue IL-17 cells stably express the IL-17RA/IL-17RC heterodimer IL-17 receptor and Act1, along with the secreted embryonic alkaline phosphatase (SEAP) reporter under the control of one NF-κB and also five AP-1 binding sites, which are regulated by MAP-kinases [45]. IL-17 binding to the IL-17 receptor triggers the ACT1-TRAF6 signaling cascade to activate NF-κB and/or AP-1 binding sites [46], which induces SEAP expression (**Figure 1A**). Following treatment with recombinant IL-17, TNF-α recombinant protein or vehicle control, SEAP was quantitated using a colorimetric assay to detect cleavage of the SEAP substrate p-Nitrophenyl phosphate [47]. As expected, TNF-α did not stimulate SEAP expression, demonstrating that the HEK-Blue IL-17 cells are specifically activated by IL-17 (data not shown). SEAP decreased more than 70% in wildtype (WT) *C. burnetii*-infected cells compared to mock- and T4BSS defective mutant (Δ*dotA*)-infected cells, indicating that *C. burnetii* inhibits IL-17 activation of the ACT1-TRAF6/NF-κB and AP-1 pathways through T4BSS effector proteins (**Figure 1B**).

Because the HEK Blue cells detect both NF-KB and MAP-kinases activation, we next assessed whether *C. burnetii* specifically targets the NF-κB and/or MAP kinase pathways following IL-17 stimulation by measuring the phosphorylation levels of NF-κB p-65, JNK/SAPK and p38 MAPK in infected mouse alveolar macrophages (MH-S cells). We observed less activation of NF-κB p-65 and p38 MAPK (**Figure 2 A and B**), and a drastic reduction in JNK/SAPK activation (**Figure 2C**) in *C. burnetii*-infected cells stimulated with

IL-17 compared to mock- or Δ*dotA* mutant-infected cells. Taken together, these data suggest that *C. burnetii* T4BSS targets both NF-κB and MAP kinase pathways, particularly JNK/SAPK, upon IL-17 stimulation as a mechanism to inhibit transcription of IL-17 downstream genes.

Disruption of the IL17R-ACT1-TRAF6 pathway neutralizes the IL-17 bactericidal effect.

Based on our findings that IL-17-stimulated macrophages kill *C. burnetii* within 24 hours [20], and our data suggesting that *C. burnetii* T4BSS downregulates the IL-17-induced activation of NF-κB and MAPK pathways (**Figure 2)**, we hypothesized that the IL-17R-ACT1-TRAF6 pathway is required for IL-17-mediated killing of *C. burnetii.* Thus, we generated IL-17RA and TRAF6 knockouts (*Δil-17ra* and *Δtraf6*) in MH-S cells (**Supplemental Figure 1**) using CRISPR/Cas9 [48] and tested *C. burnetii* survival following IL-17 treatment. As expected, in WT macrophages stimulated with IL-17 compared to untreated cells, *C. burnetii* growth was reduced by 32.7% over six days (**Figure 3A**) and the *C. burnetii*-containing vacuole (CCV) size was significantly smaller (**Figure 3B and C**). However, both bacterial replication and CCV expansion were unaffected by the presence of IL-17 in *Δil-17ra* and *Δtraf6* macrophages (**Figure 3 A-C**). Because we were unable to generate an ACT1 knockout in macrophages, we depleted ACT1 protein using siRNA (**Supplemental Figure 1**). Similarly, the fold change in recoverable bacteria over 6 days and the CCV size were sensitive to IL-17 in the control cells transfected with non-targeting siRNA (NT), but not in the siACT1 cells (**Figure 3D and E**). Intriguingly, *C. burnetii* growth improved in *Δtraf6* cells independent of IL-17, suggesting TRAF6 functions in the innate immune response against *C. burnetii*. These data indicate that the IL-17R-ACT1-TRAF6 pathway is essential for the bactericidal effect of IL-17 in macrophages.

***C. burnetii* T4BSS inhibits IL-17-mediated oxidative stress in macrophages.**

IL-17 can directly stimulate bacterial killing in both macrophages and neutrophils by enhancing their phagocytic activity as well as production of antimicrobial proteins [49-51]. Given that IL-17 can trigger reactive oxygen species (ROS) production by activating

NADPH-oxidases (NOX) through ACT1 and TRAF6 [52, 53], and the fact that high ROS levels inhibit *C. burnetii* growth [54], we hypothesized that *C. burnetii* T4BSS inhibits IL-17 signaling in macrophages to avoid elevated ROS levels. First, we tested whether IL-17 increases NOX activity in alveolar macrophages using a fluorometric assay. Following IL-17 stimulation, we detected a significant increase in NOX activity in WT cells compared to untreated cells, but there was no significant difference in *⊿il-17ra* cells treated or not with IL-17, indicating that the observed effect is due to activation of IL-17 signaling in macrophages (**Figure 4A)**. Next, using CellROX Green, we measured ROS levels in mock-, WT- and Δ*dotA* mutant-infected cells, stimulated or not with recombinant IL-17. As a positive control, uninfected cells were treated with 10 μM hydrogen peroxide. We found a significant increase of ROS levels in mock- and Δ*dotA* mutant-infected cells treated with IL-17, but not in the WT-infected cells (**Figure 4B and C**). These data suggest that *C. burnetii* employs the T4BSS to block IL-17-mediated oxidative stress to ensure its survival in macrophages.

Discussion

IL-17 is a proinflammatory cytokine that promotes the host protective innate immunity by different mechanisms, including recruiting neutrophils to the infection site and inducing IFNγ production in macrophages [55]. Our recent studies surprisingly revealed that *C. burnetii* downregulates intracellular IL-17 signaling in macrophages, using one or more T4BSS effector proteins [20]. Here, we found that *C. burnetii* T4BSS specifically blocks IL-17 activation of the NF-κB and/or MAP kinase pathways, and that the IL17R-ACT1-TRAF6 pathway is absolutely required for the bactericidal effect of IL-17. In addition, IL-17 increases ROS production in alveolar macrophages, but *C. burnetii* T4BSS inhibits this IL-17-mediated oxidative stress. Together, these data suggest that *C. burnetii* T4BSS targets intracellular pathways triggered by IL-17 to block high levels of ROS and promote bacterial survival.

Alveolar macrophages play a key role in immune surveillance of the airway and phagocytosis of inhaled bacteria before they can induce lung inflammation and pulmonary dysfunction [56]. However, different intracellular bacteria, including the highly successful pathogens *Mycobacterium tuberculosis* and *Yersinia pestis*, have evolved mechanisms

to subvert the macrophage response to alter the immune response and avoid lysosomal degradation [57-61]. Mainly spread through aerosols, *C. burnetii* initially infects alveolar macrophages, but despite the innate ability of macrophages to kill intracellular pathogens, *C. burnetii* survives, replicates, and causes disease. We recently discovered a novel mechanism used by *C. burnetii* to reduce the number of proteolytically active lysosomes available for heterotypic fusion with the CCV; this is likely a mechanism to regulate CCV acidic pH and promote bacterial survival within this harsh environment [62]. Given that *C. burnetii* infection can establish in healthy individuals with a low infectious dose (<10 organisms), the bacteria most likely employ several strategies to escape from the macrophage response during early stages of infection [63]. In fact, a functional T4BSS is absolutely required for *C. burnetii* growth in macrophages [64, 65], and different *C. burnetii* T4BSS effector proteins have been identified as key players in the immune evasion of macrophages [19, 40]. However, little information is available regarding specific innate immune pathways modulated by the *C. burnetii* during infection. As an attempt to fill this knowledge gap, we recently performed a transcriptome analysis of *C. burnetii*-infected macrophages and identified IL-17 signaling as one of the main pathways manipulated by T4BSS effector proteins. We confirmed that IL-17-target genes are downregulated in *C. burnetii*-infected cells, and found that this cytokine has a bactericidal effect, with the T4BSS mutant exhibiting significantly more sensitivity to IL-17 than WT bacteria [20]. Given that IL-17 binding to the IL-17 receptor can trigger different signaling pathways, we decided to elucidate which pathway(s) are activated and modulated by bacterial proteins in *C. burnetii*-infected macrophages upon IL-17 stimulation. We found that *C. burnetii* actively blocks the IL-17 transcriptional activation through the ACT1-TRAF6 signaling cascade, which results in NF-κB and AP-1 activation. We further confirmed downregulation of both NF-κB and MAPK pathways in *C. burnetii*-infected macrophages stimulated with IL-17. To our knowledge, this is the first report of an intracellular bacterium downregulating activation of IL-17-dependent NF-κB and MAPK pathways through bacterial effector proteins. However, previous studies have shown that both NF-κB and MAPK pathways are actively modulated by *C. burnetii* in different cells, in an IL-17-independent manner [39-41]. Interestingly, NF-κB was found to be temporally downregulated by *Coxiella* effector proteins in THP-1 cells, but inhibition of this pathway

impairs *C. burnetii* development, which indicates that *C. burnetii* maintains a balance between activation and suppression of NF-κB signaling during infection [39]. A recent study demonstrated that the *C. burnetii* effector protein NopA (nucleolar protein A) perturbs nuclear translocation of NF-κB p65 subunit and it is involved in silencing the immune response during *C. burnetii,* in U2OS cells (human bone osteosarcoma epithelial cells). However, transposon insertions in *nopA* do not affect bacterial intracellular replication [40], which suggests that additional *C. burnetii* effector proteins are likely involved in the downregulation of NF-κB signaling.

We previously found a dose-dependent decrease in *C. burnetii* viability after IL-17 treatment, with the highest concentrations killing over 50% of the bacteria [20]. Prior studies have demonstrated the bactericidal effect of IL-17 in macrophages and neutrophils [49-51]. In this study, disrupting the IL-17R-ACT1-TRAF6 signaling cascade abolished the IL-17-induced *C. burnetii* killing. IL-17 is known to activate NADPH oxidases (NOX) in an ACT1- and TRAF6-dependent manner [52, 53]. NOX causes oxidative stress by generating ROS, which has been shown to inhibit *C. burnetii* growth in macrophages [54]. Indeed, we observed increased ROS levels in IL-17-treated alveolar macrophages. Strikingly, *C. burnetii* inhibited IL-17-induced oxidative stress in a T4BSS-dependent manner. *C. burnetii* RpoS, the stationary phase factor RpoS required for bacterial survival during environmental stress [66], plays an important role in ROS resistance [67]. In addition, a recent study characterized the *C. burnetii* effector protein sdrA as a short-chain dehydrogenase, which is also essential for bacterial resistance to oxidative stress and intracellular replication [68]. While these proteins are key players in *C. burnetii's* ability to resist oxidative stress, our data suggest that there is also a T4BSS-dependent mechanism. Further investigation is needed to identify bacterial effector proteins that specifically target the IL-17R-ACT1-TRAF6 pathway in order to block excessive ROS production.

In summary, this study demonstrates that *C. burnetii* targets the IL-17R-ACT1-TRAF6 pathway to inhibit transcription of IL-17-target genes and block the activity of NOX enzymes to prevent increased ROS levels in the infected macrophages. While is not yet known which bacterial effector protein(s) are modulating both IL-17-mediated oxidative

stress, our work reveals a novel mechanism used by *C. burnetii* to evade the immune response.

Materials and Methods

Bacteria and mammalian cells.

C. burnetii Nine Mile phase II (NMII clone 4, RSA 439) wild type (WT) and *ΔdotA* mutant [69] were grown for 4 days in acidified citrate cysteine medium 2 (ACCM-2) at 37°C in 2.5% O2 and 5% CO_2, washed twice with phosphate-buffered saline (PBS), and stored as previously described [70]. Murine alveolar (MH-S) macrophages (CRL-2019; ATCC) were maintained in growth medium consisting of RPMI 1640 medium (Corning) containing 10% fetal bovine serum (FBS; Atlanta Biologicals) at 37°C in 5% CO_2. The multiplicity of infection (MOI) was optimized for each bacterial stock and culture vessel for a final infection of approximately 1 internalized bacterium per cell.

IL-17 SEAP reporter assay

Stable IL-17 promoter reporter cells (HEK-Blue™ IL-17 cells; InvivoGen) were maintained in growth medium consisting of DMEM (Dulbecco's Modified Eagle Medium; Corning) containing 10% FBS at 37°C and 5% CO_2. The cells were plated in a 6-well plate ($2x10^5$ cells per well), and after 2 days they were either mock-infected or infected with WT or *ΔdotA* mutant *C. burnetii* in 0.5 ml growth medium for 2 h, at 37°C in 5% CO_2. Infected cells were washed extensively with PBS and incubated in 2 ml growth medium. At 24 hours-post infection (hpi), cells were treated with 25 ng/ml human IL-17 recombinant protein (R&D Systems). Vehicle control or 25 ng/ml human TNF-α recombinant protein were used as controls. At 48hpi, the supernatant was collected and 20 µl was added into a white 96-well plate. The secreted embryonic alkaline phosphatase (SEAP) was measured in a microplate reader (OD Ex/Em = 620/655 nm) using Quanti-Blue Solution (InvivoGen), following the manufacturer's instructions.

Modulation of NF-κB and MAPK pathways and immunoblotting

MH-S cells were plated in a 6-well plate (2×10^5 cells per well) and allowed to adhere overnight. Cells were either mock-infected or infected with WT or *ΔdotA* mutant *C. burnetii*

in 0.5 ml RPMI 10% FBS, for 2 h. Infected cells were washed extensively with PBS and incubated in 2 ml of fresh growth medium. At 24 hpi, cells were stimulated or not with 100 ng/ml mouse IL-17 recombinant protein (R&D Systems) for 10 or 30 min. Cells were lysed with RIPA buffer (Cell Signaling Technologies) containing phosphatase and protease inhibitors (Sigma-Aldrich) and protein lysates resolved by 4-20% SDS-PAGE and transferred to nitrocellulose membrane (BioRad). The membrane was blocked in 5% milk in TBS-T (TBS containing 0.05% tween-20), for 1 h, and probed separately using the following primary rabbit antibodies (1:1000, Cell Signaling Technologies): anti-NF-κB p65 or anti-phospho NF-κB p65 (Ser536); anti-SAPK/JNK or anti-phospho SAPK/JNK (Thr183/Tyr185); and anti-p38 MAPK or anti-phospho p38 MAPK, in 5% milk in TBS-T. GAPDH was probed as a loading control (mouse anti-GAPDH. 1:1000; Thermo Fisher Scientific). After washing, the membrane was incubated for 1 h with the secondary-antibody horseradish peroxidase (HRP)- conjugated anti-rabbit or anti-mouse (1:1000; Thermo Fisher Scientific) in 5% milk in TBS-T, washed and developed using enhanced chemiluminescence (ECL) reagent (SuperSignal West Pico PLUS; Thermo Fisher Scientific). Densitometry data was done in ImageJ (Fiji) software, using the Easy Band Quantification plugin.

CRISPR/Cas9 and Real Time PCR

Disruption of the *il17ra* and *traf6* genes in MH-S cells was carried out using the CRISPR/Cas9 method [48]. An individual sgRNA was designed for each gene (IL-17RA sgRNA: GCTCTGCACCCTCGAGGTAC); (TRAF6 sgRNA: ATTTGGGCACTTTACCGTCA). The sgRNAs were prepared using the EnGen sgRNA synthesis kit following the manufacturer's protocol (New England BioLabs), and then associated with EnGen Spy Cas9 NLS protein (New England BioLabs) using the 4D-Nucleofector system (Lonza), in combination with the P3 Primary Cell 4D-Nucleofector X kit. After 48 h, the cells were cloned using a 96-well plate. *il17ra* and *traf6* clones were validated by RT-qPCR.

Protein depletion with siRNA

MH-S cells (3 x 10^5 cells/well, in a 6-well plate) were reverse transfected with 50 nM small-interfering RNA (siRNA) SMARTpool specific for mouse ACT1 (Horizon Discovery)

or non-targeting control pool (Horizon Discovery) using DharmaFECT 4 Transfection Reagent (Horizon Discovery). After 48 h, cells were infected with WT *C. burnetii,* for 2 h. Following washing with PBS, cells were harvested by trypsinization and subjected to a second round of siRNA transfection into a 24-well plate (3.5 x 10^4 cells/well). At 2 and 5 days post-infection (dpi), cells were harvested, lysed with 1x RIPA Buffer containing phosphatase and protease inhibitors, and analyzed by immunoblotting to confirm ACT1 knockdown. The membrane was probed separately using mouse anti-ACT1 (1:1000; Santa Cruz) and mouse anti-GAPDH (1:1000; Thermo Fisher Scientific) antibodies in 5% milk in TBS-T, where GAPDH was used as loading control. After washing, the blot was incubated with HRP-conjugated anti-mouse secondary antibody in 5% milk in TBS-T, and developed using enhanced chemiluminescence (ECL) reagent. Densitometry data was done in ImageJ (Fiji) software, using the Easy Band Quantification plugin.

C. burnetii intracellular growth by CFU assay

While WT, *Δil-17ra* and *Δtraf6* MH-S cells were plated in a 6-well plate (2 x 10^5 cells per well) and allowed to adhere overnight, siACT1 cells were pre-transfected 2 days before infection, as previously described. All cells were infected with WT *C burnetii* in 0.5 ml RPMI for 2 h, washed extensively with PBS, and scraped into 2 ml of fresh growth medium. Infected cells were replated in a 24-well plate (3 x 10^4 cells per well), and siACT1 cells were subjected to a second round of siRNA transfection before replating onto a 24-well plate (4 x 10^4 cells/well). Cells were stimulated with 100 ng/ml mouse IL-17 recombinant protein, and the media was changed daily to ensure constant IL-17 concentration. To determine the number of internalized bacteria at days 0 and 6, infected cells were lysed in sterile water for 5 min, diluted in ACCM-2 and spotted on 0.25% ACCM-2 agarose plates [71]. The plates were incubated for 7 to 9 days at 37°C in 2.5% O_2 and 5% CO_2, and colonies counted to measure bacterial viability. Each of the three experiments was performed in biological duplicate, and the bacteria were spotted in triplicate.

Quantification of CCV area

WT, *Δil-17ra* and *Δtraf6* MH-S cells were plated in a 6-well plate (2 x 10^5 cells per well) and allowed to adhere overnight. All cells were infected with mCherry-expressing WT *C*

burnetii in 0.5 ml RPMI for 2 h, washed extensively with PBS, and scraped into 2 ml of fresh growth medium. Infected cells were replated onto coverslips, in a 24-well plate (3×10^4 cells per well). Cells were stimulated with 100 ng/ml mouse IL-17 recombinant protein, and the media was changed daily to ensure constant IL-17 concentration. At 6 dpi, cells were fixed with 2.5% paraformaldehyde (PFA) for 15 min, washed in PBS, and blocked/permeabilized in 1% BSA and 0.1% saponin in PBS for 20 min. Coverslips were stained with rat anti-mouse LAMP1 (1:1,000; BD Biosciences) along with guinea pig anti-*C. burnetii* (1:2500) for 1 h followed by Alexa Fluor secondary antibodies (1:1,000; Invitrogen) for 1 h. Following washing with PBS, coverslips were mounted with ProLong Gold with DAPI and visualized on a Nikon eclipse Ti2 microscope, using a 60x oil immersion objective. Images were captured and processed identically, and the CCV area was measured using ImageJ (Fiji) software. At least 30 CCVs were measured per condition for each experiment.

Measurement of NADH Oxidase activity

WT and *Δil-17ra* MH-S cells were plated in a 6-well plate (2×10^5 cells per well) and allowed to adhere overnight. After 24h of IL-17 (100 ng/ml) stimulation, NOX activity was quantitated using the NADH Oxidase Activity Assay Kit (Abcam) following the manufacturer's protocol. Briefly, this fluorometric assay couples oxidation and reduction of a colorless probe to produce a brightly colored product generating fluorescence at Ex/Em = 535/587 nm. The fluorescence generated is directly proportional to the NOX activity in samples.

Detection and quantification of ROS

MH-S cells were plated in a 6-well plate (2×10^5 cells per well) and allowed to adhere overnight. Cells were infected with mCherry-expressing WT or *ΔdotA* mutant *C. burnetii,* in 0.5 ml RPMI 10% FBS, for 2 h. Infected cells were washed extensively with PBS, trypsinized, resuspended to 3×10^5 cells/ml, and plated onto ibidi-treated channel µ-slide VI0.4 (9×10^3 cells per channel; Ibidi). After 24 h, the infected cells were treated or not with 100 ng/ml mouse IL-17 recombinant protein. At 2 dpi, the cells were treated or not with 10 µM hydrogen peroxide (Thermo Fisher Scientific), and then incubated with 5 µM CellROX Green (Thermo Fisher Scientific) for 30 min. After washing with PBS, cells were

incubated in growth medium and imaged live using z-stacks of 0.3-µm steps with a Nikon spinning disk confocal microscope (60x oil immersion objective). Images were captured and processed identically; fluorescence intensity was measured using ImageJ (Fiji) software.

Data analyses

Image processing and analyses were done in ImageJ (Fiji) software. Statistical analyses were performed using an unpaired Student's t test, ordinary one-way ANOVA (with Tukey's correction), or multiple t tests as appropriate in Prism (GraphPad). Model figure was made using Biorender.

Acknowledgements

We thank Seth Winfree, Rey Carabeo, and members of the Gilk Lab for helpful discussions and critical feedback. This research was supported by National Institutes of Health (1R21AI149723-01A1) (SDG) and an American Heart Association Postdoctoral Fellowship (834525) (TMC). We have no conflicts of interest to declare.

Figure legends

Figure 1. ***C. burnetii*** **T4BSS blocks IL-17-induced transcription (A)** HEK-Blue IL-17 SEAP reporter cells stably express the IL-17RA/IL-17RC heterodimer receptor and Act1, along with the secreted embryonic alkaline phosphatase (SEAP) reporter under the control of one NF-κB and five AP-1 (MAPK pathway) binding sites. IL-17 binding to the IL-17 receptor triggers the ACT1-TRAF6 signaling cascade, leading to SEAP transcription. **(B)** HEK-Blue IL-17 SEAP reporter cells were infected for 24h, followed by IL-17 treatment (25 ng/mL) for 24h. SEAP concentration was determined by the colorimetric enzyme assay QUANTI-Blue; a robust induction of SEAP upon IL-17 stimulation was measured in mock- and *ΔdotA* mutant-infected cells, but infection with *C. burnetii* decreased SEAP by 72.3%, suggesting that *C. burnetii* inhibits the IL-17 transcriptional activation pathway. Data shown as means ± SEM from three independent experiments. Statistical significance was determined by one-way ANOVA with Tukey's multiple comparisons test, *p<0.05, **p<0.01.

Figure 2. *C. burnetii* T4BSS blocks IL-17 activation of NF-κB p65, MAPK, and SAPK/JNK pathways. Representative immunoblots of lysates from MH-S either mock-infected or infected with WT or *ΔdotA* mutant *C. burnetii.* Densitometry analysis as indicated by numbers between panels shows decreased phosphorylated levels of **(A)** NF-κB p65 (Ser536), **(B)** p38-MAPK and **(C)** SAPK/JNK (Thr183/Tyr185) in wildtype-infected cells compared to mock- and *ΔdotA* mutant-infected cells. GAPDH was used as loading control.

Figure 3. **Disruption of the IL17R-ACT1-TRAF6 pathway neutralizes the IL-17 bactericidal effect.** Stimulation with IL-17 (100 ng/ml) negatively affects *C. burnetii* growth in **(A)** WT MH-S cells or **(D)** control non-targeting siRNA (NT) cells, but not in the **(A)** CRISPR knockouts (*⊿il-17ra* and *⊿traf6*) or **(D)** siACT1 MH-S cells, indicating that the bactericidal effect of IL-17 relies on the IL17R-ACT1-TRAF6 pathway. Viable bacteria were quantitated after 6 days using an agarose-based CFU assay, and p values determined by two-way ANOVA, *p<0.05, **p<0.01. **(C)** Immunofluorescence staining and **(B and E)** quantitative measurements indicate that CCVs are significantly smaller in WT cells treated with IL-17, but their size is not affected by IL17 in *⊿il-17ra, ⊿traf6,* or siACT1 infected-cells. Representative images of CCVs stained by immunofluorescence at 6 dpi (days post infection; scale bar: 10μM). Blue, DAPI (host cell nuclei); green, LAMP1 (lysosomes and CCV); red, *C. burnetii*. CCV size was measured using ImageJ, with each circle representing an individual CCV. Data are shown as the mean ± SEM of at least 60 cells from independent experiments. Statistical significance was determined by two-way ANOVA, ****p<0.001.

Figure 4. *C. burnetii* blocks IL-17-induced ROS generation through T4BSS effector proteins. (A) IL-17 increases NADH oxidase (NOX) activity in MH-S macrophages. WT and *⊿il-17ra* MH-S cells were treated or not with recombinant IL-17 (100 ng/ml) and the NOX activity was measured. IL-17 stimulation significantly increased NOX activity WT cells, but not in *il-17ra* cells. Data shown as means ± SEM from three independent experiments. Statistical significance was determined by one-way ANOVA with Tukey's

multiple comparisons test, ***p<0.005. **(B)** MH-S cells were infected with mCherry-expressing WT or *ΔdotA* mutant bacteria, treated or not with recombinant IL-17 (100 ng/ml) and ROS levels were stained with CellROX Green at 2 dpi. Z-stacks were acquired by live cell spinning disk microscopy. As a positive control, mock-infected cells were treated for 2 h with 10 µM H_2O_2. ROS levels are shown as a heat map on the far right column, with green showing high levels of ROS and blue showing low levels of ROS (scale bar: 10µM). **(C)** Measurements of ROS were obtained using ImageJ and normalized to the cell area. Stimulation with IL-17 significantly increased the ROS levels in mock- and *ΔdotA* mutant-infected, but not in WT-infected cells, suggesting that *C. burnetii* T4BSS blocks IL-17-induced ROS production in macrophages. Data are shown as the mean ± SEM of at least 30 cells per condition in each of three independent experiments. Statistical significance was determined by one-way ANOVA with Tukey's post hoc test, *p<0.05, **p<0.01.

Supplementary Figure 1. Depletion of *il-17ra, traf6* and ACT1 in MH-S cells. (A-B) Quantitative expression of *il-17ra* and *traf6* in MH-S cells by real time PCR using specific primers confirmed knockout of *il-17ra* and *traf6* using CRISPR-Cas9. **(C)** Immunoblot revealed the depletion of ACT1 in MH-S using siRNA. Control cells were transfected with non-targeting siRNA (NT).

References

1. Maurin, M. and D. Raoult, *Q fever.* Clin Microbiol Rev, 1999. **12**(4): p. 518-53.
2. Rahaman, M.R., et al., *Is a One Health Approach Utilized for Q Fever Control? A Comprehensive Literature Review.* Int J Environ Res Public Health, 2019. **16**(5).
3. Million, M., et al., *Evolution from acute Q fever to endocarditis is associated with underlying valvulopathy and age and can be prevented by prolonged antibiotic treatment.* Clin Infect Dis, 2013. **57**(6): p. 836-44.
4. Kampschreur, L.M., et al., *Chronic Q fever diagnosis— consensus guideline versus expert opinion.* Emerg Infect Dis, 2015. **21**(7): p. 1183-8.
5. Raoult, D., *Treatment of Q fever.* Antimicrob Agents Chemother, 1993. **37**(9): p. 1733-6.

6. Dahlgren, F.S., D.L. Haberling, and J.H. McQuiston, *Q fever is underestimated in the United States: a comparison of fatal Q fever cases from two national reporting systems.* Am J Trop Med Hyg, 2015. **92**(2): p. 244-6.

7. Maor, Y., et al., *Coxiella burnetii Endocarditis and Aortic Vascular Graft Infection: An Underrecognized Disease.* Ann Thorac Surg, 2016. **101**(1): p. 141-5.

8. Keijmel, S.P., et al., *A fatal case of disseminated chronic Q fever: a case report and brief review of the literature.* Infection, 2016. **44**(5): p. 677-82.

9. Botelho-Nevers, E., et al., *Coxiella burnetii infection of aortic aneurysms or vascular grafts: report of 30 new cases and evaluation of outcome.* Eur J Clin Microbiol Infect Dis, 2007. **26**(9): p. 635-40.

10. Parker, N.R., J.H. Barralet, and A.M. Bell, *Q fever.* Lancet, 2006. **367**(9511): p. 679-88.

11. Kampschreur, L.M., et al., *Screening for Coxiella burnetii seroprevalence in chronic Q fever high-risk groups reveals the magnitude of the Dutch Q fever outbreak.* Epidemiol Infect, 2013. **141**(4): p. 847-51.

12. Bjork, A., et al., *First reported multistate human Q fever outbreak in the United States, 2011.* Vector Borne Zoonotic Dis, 2014. **14**(2): p. 111-7.

13. Bamberg, W.M., et al., *Outbreak of Q fever associated with a horse-boarding ranch, Colorado, 2005.* Vector Borne Zoonotic Dis, 2007. **7**(3): p. 394-402.

14. Nett, R.J., S.D. Helgerson, and A.D. Anderson, *Clinician assessment for Coxiella burnetii infection in hospitalized patients with potentially compatible illnesses during Q fever outbreaks and following a health alert, Montana, 2011.* Vector Borne Zoonotic Dis, 2013. **13**(2): p. 128-30.

15. Alonso, E., et al., *Q Fever Outbreak among Workers at a Waste-Sorting Plant.* PLoS One, 2015. **10**(9): p. e0138817.

16. Porter, S.R., et al., *Q fever in Japan: an update review.* Vet Microbiol, 2011. **149**(3-4): p. 298-306.

17. Amitai, Z., et al., *A large Q fever outbreak in an urban school in central Israel.* Clin Infect Dis, 2010. **50**(11): p. 1433-8.

18. Voth, D.E., D. Howe, and R.A. Heinzen, *Coxiella burnetii inhibits apoptosis in human THP-1 cells and monkey primary alveolar macrophages.* Infect Immun, 2007. **75**(9): p. 4263-71.

19. Cunha, L.D., et al., *Inhibition of inflammasome activation by Coxiella burnetii type IV secretion system effector IcaA.* Nat Commun, 2015. **6**: p. 10205.

509 20. Clemente, T.M., et al., *Coxiella burnetii Blocks Intracellular Interleukin-17 Signaling*
510 *in Macrophages.* Infect Immun, 2018. **86**(10).

511 21. Curtis, M.M. and S.S. Way, *Interleukin-17 in host defence against bacterial,*
512 *mycobacterial and fungal pathogens.* Immunology, 2009. **126**(2): p. 177-85.

513 22. Khader, S.A. and R. Gopal, *IL-17 in protective immunity to intracellular pathogens.*
514 Virulence, 2010. **1**(5): p. 423-7.

515 23. Onishi, R.M. and S.L. Gaffen, *Interleukin-17 and its target genes: mechanisms of*
516 *interleukin-17 function in disease.* Immunology, 2010. **129**(3): p. 311-21.

517 24. Amatya, N., A.V. Garg, and S.L. Gaffen, *IL-17 Signaling: The Yin and the Yang.*
518 Trends Immunol, 2017. **38**(5): p. 310-322.

519 25. McGeachy, M.J., D.J. Cua, and S.L. Gaffen, *The IL-17 Family of Cytokines in Health*
520 *and Disease.* Immunity, 2019. **50**(4): p. 892-906.

521 26. Bazett, M., M.E. Bergeron, and C.K. Haston, *Streptomycin treatment alters the*
522 *intestinal microbiome, pulmonary T cell profile and airway hyperresponsiveness in a*
523 *cystic fibrosis mouse model.* Sci Rep, 2016. **6**: p. 19189.

524 27. Tan, H.L., et al., *The Th17 pathway in cystic fibrosis lung disease.* Am J Respir Crit
525 Care Med, 2011. **184**(2): p. 252-8.

526 28. Kolls, J.K. and A. Lindén, *Interleukin-17 family members and inflammation.* Immunity,
527 2004. **21**(4): p. 467-76.

528 29. Barin, J.G., et al., *Macrophages participate in IL-17-mediated inflammation.* Eur J
529 Immunol, 2012. **42**(3): p. 726-36.

530 30. Lin, Y., et al., *Interleukin-17 is required for T helper 1 cell immunity and host*
531 *resistance to the intracellular pathogen Francisella tularensis.* Immunity, 2009. **31**(5):
532 p. 799-810.

533 31. Kimizuka, Y., et al., *Roles of interleukin-17 in an experimental Legionella*
534 *pneumophila pneumonia model.* Infect Immun, 2012. **80**(3): p. 1121-7.

535 32. Chen, J., et al., *IL-17A induces pro-inflammatory cytokines production in*
536 *macrophages via MAPKinases, NF-κB and AP-1.* Cell Physiol Biochem, 2013. **32**(5):
537 p. 1265-74.

538 33. Gu, C., L. Wu, and X. Li, *IL-17 family: cytokines, receptors and signaling.* Cytokine,
539 2013. **64**(2): p. 477-85.

540 34. Leonardi, A., et al., *CIKS, a connection to Ikappa B kinase and stress-activated*
541 *protein kinase.* Proc Natl Acad Sci U S A, 2000. **97**(19): p. 10494-9.

35. Toy, D., et al., *Cutting edge: interleukin 17 signals through a heteromeric receptor complex.* J Immunol, 2006. **177**(1): p. 36-9.

36. Jin, W. and C. Dong, *IL-17 cytokines in immunity and inflammation.* Emerg Microbes Infect, 2013. **2**(9): p. e60.

37. Novatchkova, M., et al., *The STIR-domain superfamily in signal transduction, development and immunity.* Trends Biochem Sci, 2003. **28**(5): p. 226-9.

38. Chang, S.H., H. Park, and C. Dong, *Act1 adaptor protein is an immediate and essential signaling component of interleukin-17 receptor.* J Biol Chem, 2006. **281**(47): p. 35603-7.

39. Mahapatra, S., et al., *Coxiella burnetii Employs the Dot/Icm Type IV Secretion System to Modulate Host NF-κB/RelA Activation.* Front Cell Infect Microbiol, 2016. **6**: p. 188.

40. Burette, M., et al., *Modulation of innate immune signaling by a Coxiella burnetii eukaryotic-like effector protein.* Proc Natl Acad Sci U S A, 2020. **117**(24): p. 13708-13718.

41. Voth, D.E. and R.A. Heinzen, *Sustained activation of Akt and Erk1/2 is required for Coxiella burnetii antiapoptotic activity.* Infect Immun, 2009. **77**(1): p. 205-13.

42. Jansen, A.F.M., et al., *Viable Coxiella burnetii Induces Differential Cytokine Responses in Chronic Q Fever Patients Compared to Heat-Killed Coxiella burnetii.* Infect Immun, 2018. **86**(10).

43. Ammerdorffer, A., et al., *Coxiella burnetii isolates originating from infected cattle induce a more pronounced proinflammatory cytokine response compared to isolates from infected goats and sheep.* Pathog Dis, 2017. **75**(4).

44. Elliott, A., et al., *Neutrophils play an important role in protective immunity against Coxiella burnetii infection.* Infect Immun, 2015. **83**(8): p. 3104-13.

45. Whitmarsh, A.J. and R.J. Davis, *Transcription factor AP-1 regulation by mitogen-activated protein kinase signal transduction pathways.* J Mol Med (Berl), 1996. **74**(10): p. 589-607.

46. Monin, L. and S.L. Gaffen, *Interleukin 17 Family Cytokines: Signaling Mechanisms, Biological Activities, and Therapeutic Implications.* Cold Spring Harb Perspect Biol, 2018. **10**(4).

47. Lorenz, U., *Protein tyrosine phosphatase assays.* Curr Protoc Immunol, 2011. **Chapter 11**: p. Unit 11.7.

48. Ran, F.A., et al., *Genome engineering using the CRISPR-Cas9 system.* Nat Protoc, 2013. **8**(11): p. 2281-2308.

576 49. Lu, Y.J., et al., *Interleukin-17A mediates acquired immunity to pneumococcal*
577 *colonization.* PLoS Pathog, 2008. **4**(9): p. e1000159.

578 50. Zhang, Q., et al., *IL-17-mediated M1/M2 macrophage alteration contributes to*
579 *pathogenesis of bisphosphonate-related osteonecrosis of the jaws.* Clin Cancer Res,
580 2013. **19**(12): p. 3176-88.

581 51. Liang, S.C., et al., *Interleukin (IL)-22 and IL-17 are coexpressed by Th17 cells and*
582 *cooperatively enhance expression of antimicrobial peptides.* J Exp Med, 2006.
583 **203**(10): p. 2271-9.

584 52. Huang, H., et al., *IL-17 stimulates the proliferation and differentiation of human*
585 *mesenchymal stem cells: implications for bone remodeling.* Cell Death Differ, 2009.
586 **16**(10): p. 1332-43.

587 53. Pietrowski, E., et al., *Pro-inflammatory effects of interleukin-17A on vascular smooth*
588 *muscle cells involve NAD(P)H- oxidase derived reactive oxygen species.* J Vasc Res,
589 2011. **48**(1): p. 52-8.

590 54. Brennan, R.E., et al., *Both inducible nitric oxide synthase and NADPH oxidase*
591 *contribute to the control of virulent phase I Coxiella burnetii infections.* Infect Immun,
592 2004. **72**(11): p. 6666-75.

593 55. Mills, K.H.G., *IL-17 and IL-17-producing cells in protection versus pathology.* Nat Rev
594 Immunol, 2023. **23**(1): p. 38-54.

595 56. Neupane, A.S., et al., *Patrolling Alveolar Macrophages Conceal Bacteria from the*
596 *Immune System to Maintain Homeostasis.* Cell, 2020. **183**(1): p. 110-125.e11.

597 57. Deretic, V., et al., *Mycobacterium tuberculosis inhibition of phagolysosome*
598 *biogenesis and autophagy as a host defence mechanism.* Cell Microbiol, 2006. **8**(5):
599 p. 719-27.

600 58. Cohen, S.B., et al., *Alveolar Macrophages Provide an Early Mycobacterium*
601 *tuberculosis Niche and Initiate Dissemination.* Cell Host Microbe, 2018. **24**(3): p. 439-
602 446.e4.

603 59. Cambier, C.J., et al., *Phenolic Glycolipid Facilitates Mycobacterial Escape from*
604 *Microbicidal Tissue-Resident Macrophages.* Immunity, 2017. **47**(3): p. 552-565.e4.

605 60. Chandra, P., S.J. Grigsby, and J.A. Philips, *Immune evasion and provocation by*
606 *Mycobacterium tuberculosis.* Nat Rev Microbiol, 2022. **20**(12): p. 750-766.

607 61. Banerjee, S.K., et al., *Modeling Pneumonic Plague in Human Precision-Cut Lung*
608 *Slices Highlights a Role for the Plasminogen Activator Protease in Facilitating Type*
609 *3 Secretion.* Infect Immun, 2019. **87**(8).

610 62. Samanta, D., et al., *Coxiella burnetii Type 4B Secretion System-dependent*
611 *manipulation of endolysosomal maturation is required for bacterial growth.* PLoS
612 Pathog, 2019. **15**(12): p. e1007855.

613 63. Brooke, R.J., et al., *Human dose response relation for airborne exposure to Coxiella*
614 *burnetii.* BMC Infect Dis, 2013. **13**: p. 488.

615 64. Carey, K.L., et al., *The Coxiella burnetii Dot/Icm system delivers a unique repertoire*
616 *of type IV effectors into host cells and is required for intracellular replication.* PLoS
617 Pathog, 2011. **7**(5): p. e1002056.

618 65. Beare, P.A., et al., *Dot/Icm type IVB secretion system requirements for Coxiella*
619 *burnetii growth in human macrophages.* mBio, 2011. **2**(4): p. e00175-11.

620 66. Dong, T. and H.E. Schellhorn, *Role of RpoS in virulence of pathogens.* Infect Immun,
621 2010. **78**(3): p. 887-97.

622 67. Moormeier, D.E., et al., *Coxiella burnetii RpoS Regulates Genes Involved in*
623 *Morphological Differentiation and Intracellular Growth.* J Bacteriol, 2019. **201**(8).

624 68. Bitew, M.A., et al., *SdrA, an NADP(H)-regenerating enzyme, is crucial for Coxiella*
625 *burnetii to resist oxidative stress and replicate intracellularly.* Cell Microbiol, 2020.
626 **22**(5): p. e13154.

627 69. Beare, P.A., et al., *Two systems for targeted gene deletion in Coxiella burnetii.* Appl
628 Environ Microbiol, 2012. **78**(13): p. 4580-9.

629 70. Omsland, A., et al., *Host cell-free growth of the Q fever bacterium Coxiella burnetii.*
630 Proc Natl Acad Sci U S A, 2009. **106**(11): p. 4430-4.

631 71. Vallejo Esquerra, E., et al., *Physicochemical and Nutritional Requirements for Axenic*
632 *Replication Suggest Physiological Basis for Coxiella burnetii Niche Restriction.* Front
633 Cell Infect Microbiol, 2017. **7**: p. 190.
634

Figure 1

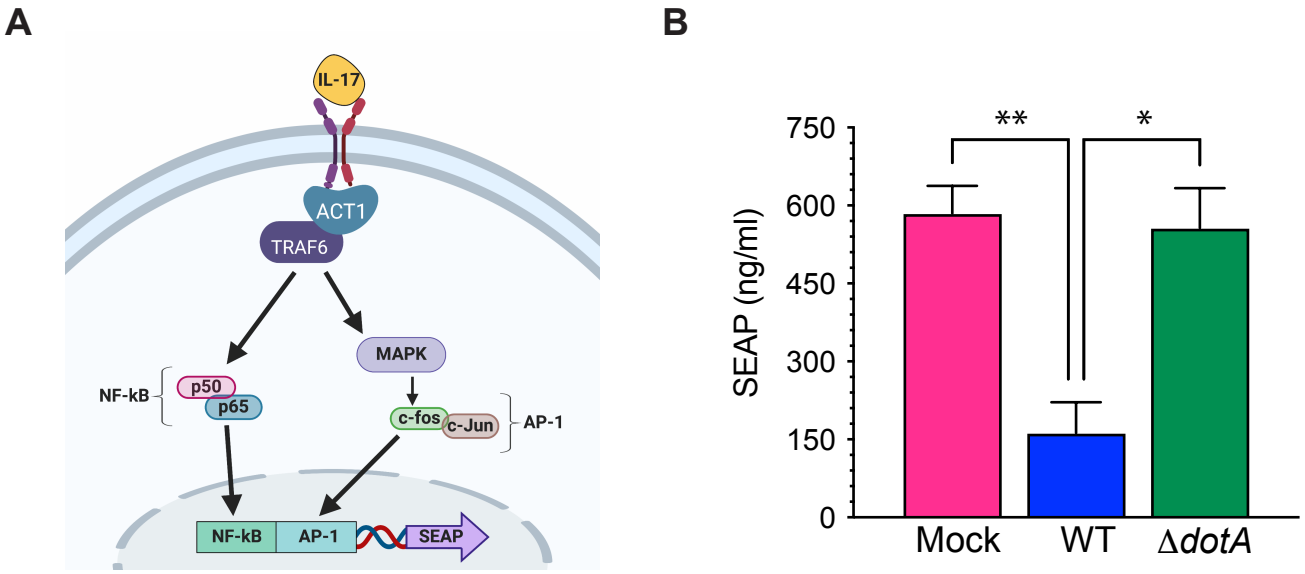

Figure 2

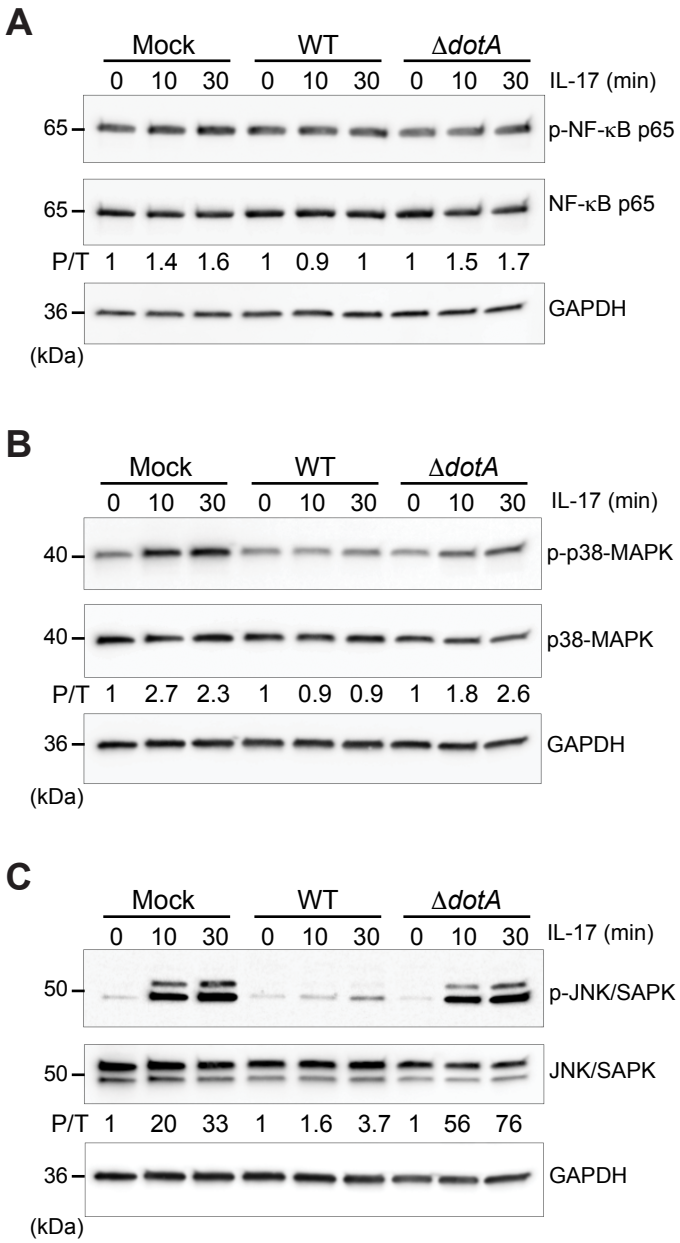

Figure 3

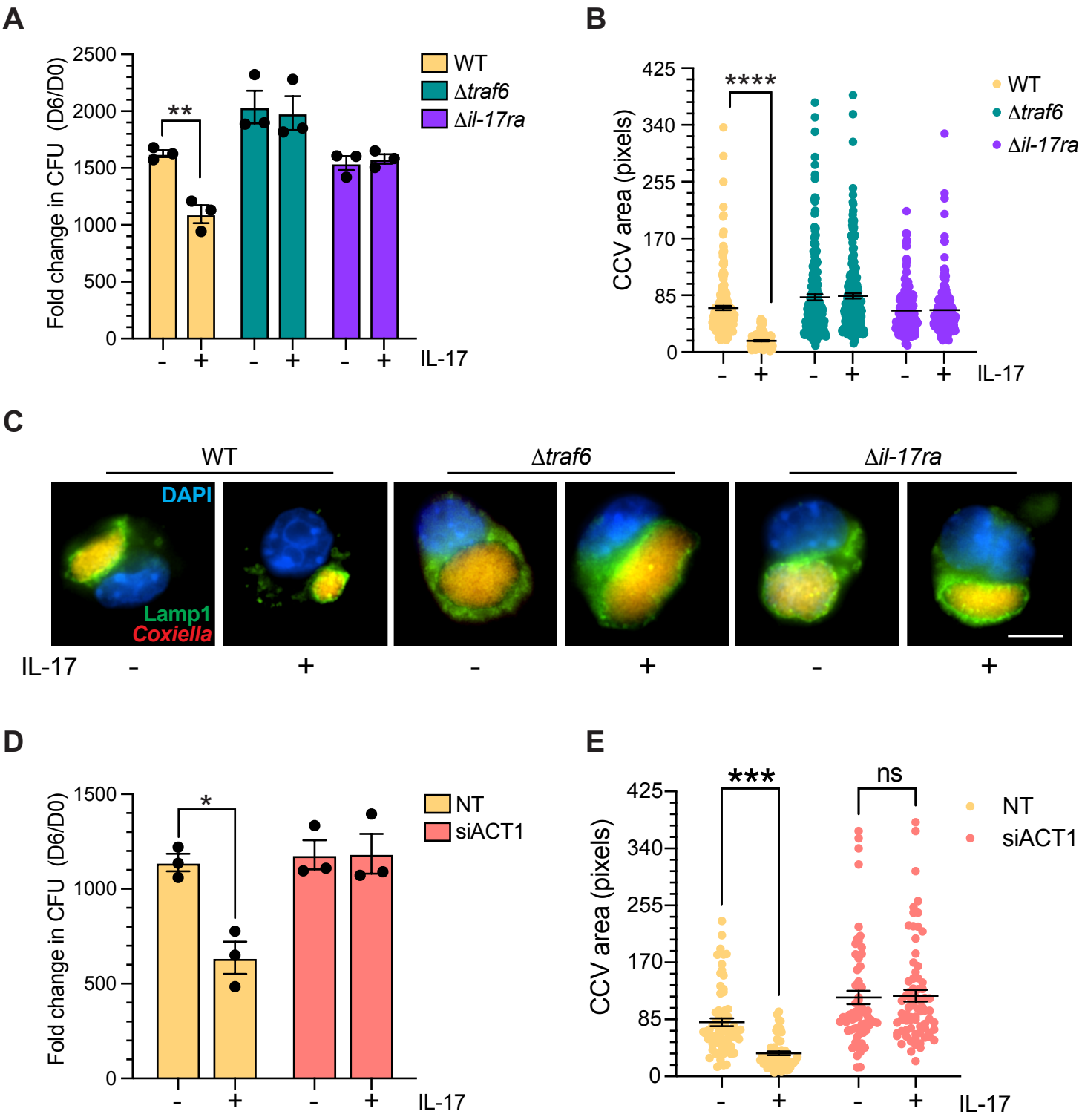

Figure 4

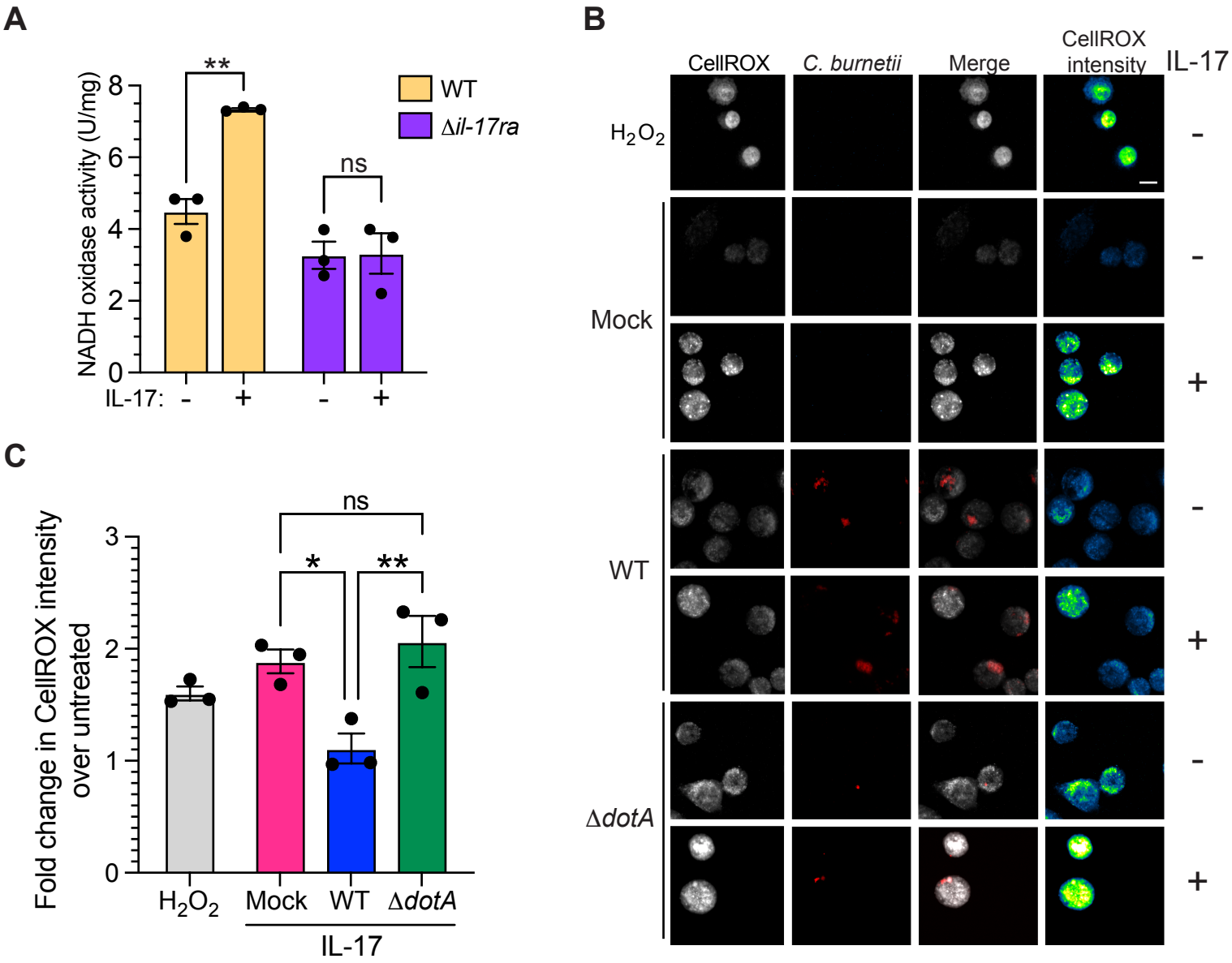

Supplementary Figure 1